

DIFFUSION OF IMPURITIES FROM ION IMPLANTS IN SILICON

A Thesis Presented in Partial Fulfillment of the Requirements

for the

Degree of Master of Science

at

Lakehead University

Janis Rozenbergs

Lakehead University

1974

ProQuest Number: 10611590

All rights reserved

INFORMATION TO ALL USERS

The quality of this reproduction is dependent upon the quality of the copy submitted.

In the unlikely event that the author did not send a complete manuscript and there are missing pages, these will be noted. Also, if material had to be removed, a note will indicate the deletion.



ProQuest 10611590

Published by ProQuest LLC (2017). Copyright of the Dissertation is held by the Author.

All rights reserved.

This work is protected against unauthorized copying under Title 17, United States Code
Microform Edition © ProQuest LLC.

ProQuest LLC.
789 East Eisenhower Parkway
P.O. Box 1346
Ann Arbor, MI 48106 - 1346

THESES

M.Sc

1975

.R89

C.1



© Janis Rozenbergs 1976

214947

PARTIAL PUBLICATION OF MATERIAL USED IN THIS THESIS

Some of the data presented in this thesis has been published in a paper by: H. Heinrich, L. Hastings and J. Rozenbergs, entitled: *Simultaneous Diffusion of Ion-predeposited As and B in Silicon*, in the Journal of Applied Physics, October 1974.

ABSTRACT

The use of shallow single and double impurity ion implants as diffusion sources was studied on bare (111) silicon wafers implanted at room temperature with 45 KeV boron, phosphorus and arsenic. The samples were diffused in a vacuum from 900°C to 1100°C. The experimental diffusion profiles were well approximated by a gaussian distribution, except near the surface. It was determined that for single diffusions about 50% of the arsenic, 60% of the phosphorus and all of the boron ions became electrically active after diffusion. Within experimental error, there was no interaction evident between the simultaneously diffusing arsenic and boron. The values of the diffusion coefficients obtained were within the wide range of values quoted in the literature.

ACKNOWLEDGEMENTS

I would like to express my gratitude to Dr. Helmut Heinrich and Dr. Lynden Hastings for their valuable assistance in my work and in the preparation of this thesis.

I would also like to thank Professor B. J. Spenceley and Dr. W. J. Keeler for their helpful comments.

LIST OF FIGURES

	[PAGE]
Figure 1	Main features of an idealized semi-logarithmic concentration profile of a single n-type impurity diffusion into a p-type substrate 4
Figure 2	Main features of an idealized semi-logarithmic profile of a double diffusion 5
Figure 3	Sheet resistivity <i>versus</i> depth profile using a four point probe in conjunction with anodic oxidation profiling 9
Figure 4	The concentration <i>versus</i> depth profile derived from the sheet resistivity profile in Fig. 3 11
Figure 5	Schematic diagram of ion accelerator 13
Figure 6	Diagram of target chamber and sample holder 15
Figure 7	Diagram of anodic oxidation arrangement 18
Figure 8	Diagram of angle polishing arrangement 20
Figure 9	Per cent of implanted dose that became electrically active after a diffusion of 900°C for various diffusion times 23
Figure 10	Angle lapped and stained samples showing the carrier type distribution. The dark regions are p-type silicon 25
Figure 11	The junction depths obtained by the anodic oxidation - sheet resistivity method, after a diffusion at 900°C for various diffusion times 27

Figure 12	Junction depths for boron diffusions in n-type silicon obtained by anodic oxidation profiling after a diffusion time of 4 hours at various diffusion temperatures	28
Figure 13	Junction depths for arsenic diffusions in p-type silicon obtained by anodic profiling after a diffusion time of 4 hours at various diffusion temperatures	29
Figure 14	Typical sheet resistivity <i>versus</i> depth profile of a double diffusion of arsenic and boron in n-type silicon. The measurements were obtained using the four point probe and anodic oxidation arrangement	31
Figure 15	The concentration profile derived from the resistivity profile in Fig. 14. The best fitting gaussian curves are represented by dot and dash curves	32
Figure 16	The experimental points and calculated profiles for boron after a diffusion of 4 hours	37
Figure 17	The diffusion coefficients for single impurity diffusions at various diffusion temperatures, obtained by fitting the gaussian distribution profile to the obtained results. The curves are due to Fuller and Ditzenberger (1956)	40

LIST OF TABLES

[PAGE]

Table 1	Comparison of the implanted dose and parameters of the best fitting gaussian profiles for the doubly implanted and simultaneously diffused sample in Fig. 15	35
Table 2	Comparison of the implanted dose and parameters of the best fitting gaussian profiles for the boron concentration profiles in Fig. 17	38

TABLE OF CONTENTS

	[PAGE]
Abstract	<i>i</i>
Acknowledgements	<i>ii</i>
List of Figures	<i>iii</i>
List of Tables	<i>v</i>
INTRODUCTION	1
THEORY	3
■ Determination of the Impurity Concentration Profiles	7
EXPERIMENTAL PROCEDURE	12
■ Sample Preparation	12
■ Implantation	12
■ Diffusion	14
■ Formation of the Mesa Structure	16
■ Sheet Resistivity Measurements	16
■ Anodic Oxidation	17
■ Visual Measurement of Junction Depth	19
RESULTS AND DISCUSSION	22
■ Sources of Errors and Accuracy	39
CONCLUSIONS	43
REFERENCES	45

INTRODUCTION

Ion implantation as a means of doping semiconductor materials has received much attention in the last five to ten years. The idea of implanting impurity atoms into semiconductors is not new. As early as 1952 doping effects were observed when semiconductors were bombarded by energetic heavy ions (Ohl 1952). Consequently, with the demand for more precise doping of semiconductors in the early 60's, the interest in ion implantation intensified.

Some of the advantages of ion implantation over thermal doping are lower process temperatures, a greater variety of dopants, the possibility of attaining doping concentrations well above the solid solubility limit, and a greater reproducibility of depth of introduced ions. Ion implantation can also be used as a convenient method of introducing material as a source for diffusion and in fact has recently been used in semiconductor technology (Wagner 1972).

The present work was undertaken to investigate the possibility of obtaining multiple layers of alternating charge carrier type by a single diffusion process. The idea of simultaneously diffusing several dopants with proper diffusion coefficients and donor and acceptor qualities to obtain such a multilayer structure has been suggested in the past (Duncan 1972).

There have been several methods used for the simultaneous diffusion of different types of impurities. The use of platelets of semiconductors and amorphous semiconductor layers as sources of diffusion have not shown favourable potential for integrated circuit manufacture.

With these methods, the reproducibility of the dose and the spatial distribution have been difficult to control. With ion implantation, the possibility of controlling the dose and the depth of introduced ions of single impurities has already been recognized (Baron, Shifrin, Marsh and Mayer 1969).

Silicon is particularly suited for simultaneous diffusion of multiple dopants. The diffusion coefficients (at 1100°C) for example of Sb, In P and Al each differ approximately by a factor of 3 from the adjacent element. A simultaneous diffusion of these elements in n-type Si would yield a four layer structure.

In this work, n-type silicon has been bombarded with As and B ions and diffused simultaneously to form an n-p-n structure. The impurity concentration profiles of singly implanted and diffused phosphorus, boron and arsenic atoms were also investigated. In particular, the effects of diffusion temperature and time, and implanted dose on the concentration profile were noted. The samples were analyzed by angle lapping and staining, as well as by sheet resistivity measurements made in conjunction with profiling by anodic oxidation. A comparison of the results obtained after diffusion of single and double implanted samples was made to determine any interaction between the two simultaneously diffusing impurities.

THEORY

This study is concerned with the diffusion of p-type and n-type impurities into silicon with a homogeneous bulk concentration of n-type phosphorus impurity or p-type boron impurity. It is assumed that the impurity is introduced into a thin surface layer by ion implantation. This layer acts as a source for diffusion. After diffusion the result is a p-n or n-p junction at a depth where the concentration of the diffusing impurity is equal to the bulk concentration of the opposite charge impurity. Fig. 1 shows, for example, the case of an n-type diffusion into a p-type wafer. In this figure, the impurity concentration along the vertical axis is a logarithmic scale, while the horizontal axis which represents the depth from the surface is a linear scale. From the surface to the junction depth (represented by the broken line), the diffusing n-type impurity dominates and compensates the p-type background impurity, resulting in n-type silicon. On the right, the background impurity concentration dominates and the silicon here remains p-type.

If a p- and an n-type impurity are diffused simultaneously, a double junction will be formed under the condition that there is an appreciable difference between the diffusion coefficients of the two impurities and that the silicon wafer is of opposite conductivity type to the fastest diffusing impurity. If the n- and p-type impurities diffuse independently of one another, a semilogarithmic plot of concentration *versus* depth as in Fig. 2 will be obtained. In this figure, the dotted line represents the net difference between the acceptor-type impurities and the donor-

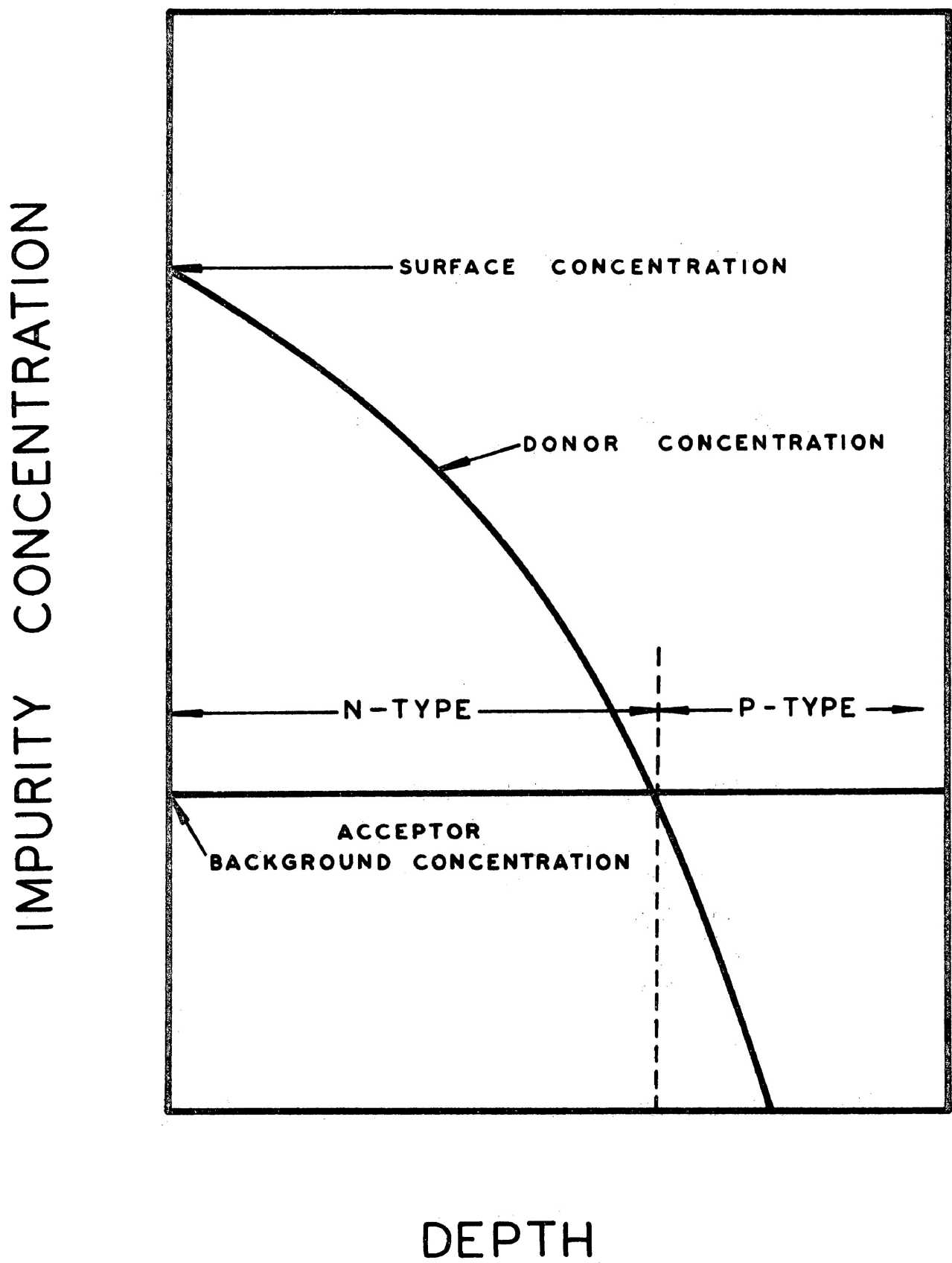


Figure 1. Main features of an idealized semi-logarithmic concentration profile of a single n-type impurity diffusion into a p-type substrate.

IMPURITY CONCENTRATION

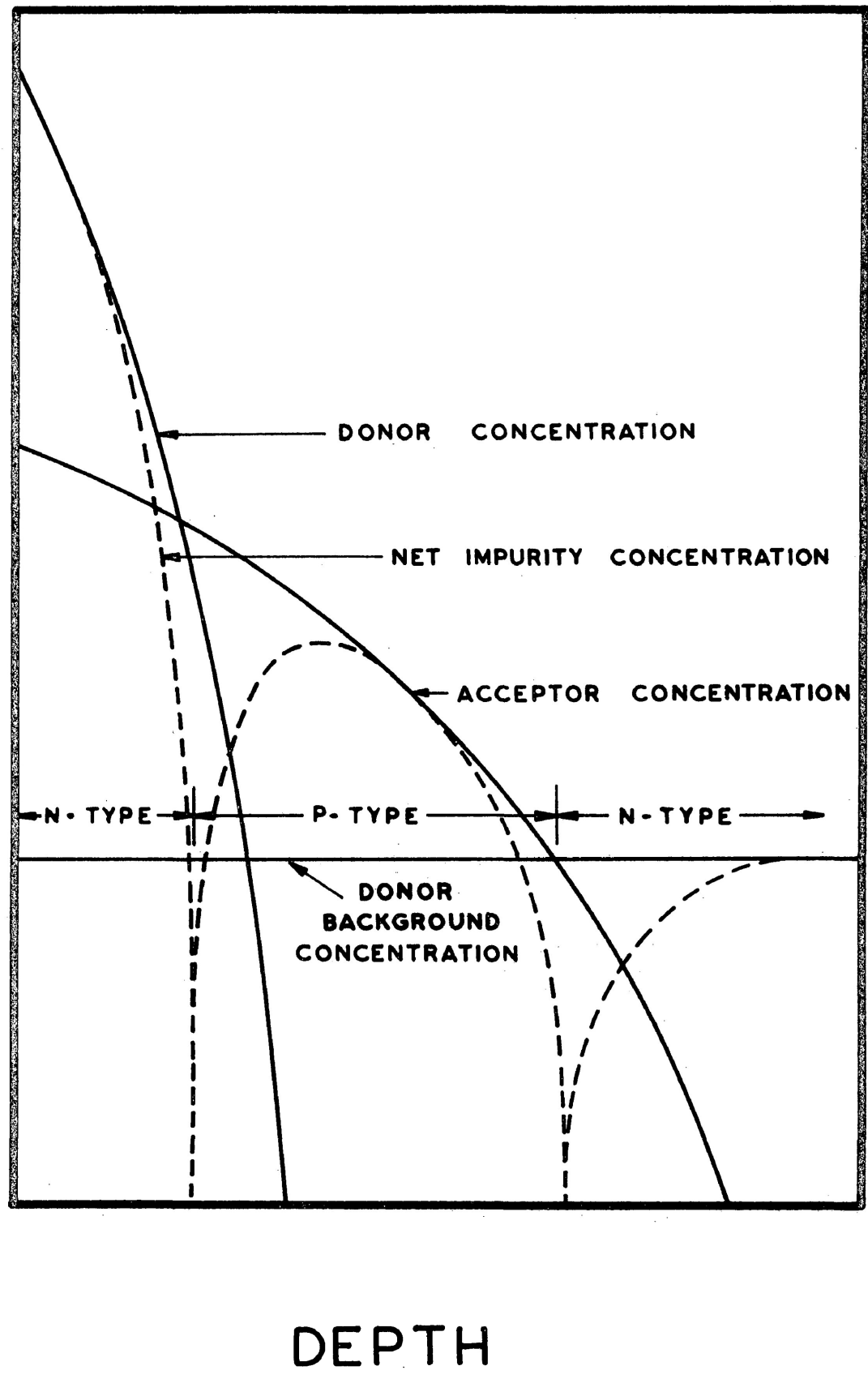


Figure 2. Main features of an idealized semi-logarithmic profile of a double diffusion.

type impurities, i.e. $N_A \dots N_D$.

Diffusion is fairly well understood and treatments of the subject may be found in texts (see, for example, Shewmon 1963).

In the simple theory of diffusion one can assume that an impurity will diffuse independently of any other type of impurity and that the rate of diffusion is independent of concentration. Both of these assumptions are not rigorously true, but are accurate enough for many calculations.

Fick's first law states that the amount of material diffusing per unit time, \vec{J} , is related to the concentration gradient, $\vec{\nabla}N$, by the factor of proportionality, D , the diffusion coefficient:

$$\vec{J} = - D \vec{\nabla} N .$$

For the one-dimensional case, Fick's first law may be written as:

$$J = - D \frac{\partial N}{\partial x} .$$

where x is the direction in which diffusion proceeds.

If one considers the effect of non-steady state conditions on the diffusion of an impurity into a semiconductor, Fick's second law of diffusion is obtained:

$$\frac{\partial N}{\partial t} = \frac{\partial}{\partial x} \left(D \frac{\partial N}{\partial x} \right) .$$

If D is independent of concentration, then Fick's second law becomes:

$$\frac{\partial N}{\partial t} = D \frac{\partial^2 N}{\partial x^2} .$$

There has been much analysis of this linear differential equation in books of diffusion, with a great variety of initial and boundary

conditions (Carslaw, Jaegar 1948; Crank 1956).

If the assumption is made that a finite amount of impurity ions per unit area (Q) has been deposited on the surface of the sample and then heated in an atmosphere which prevents the evaporation of the impurity ions from the surface, diffusion will take place which will have a gaussian shaped concentration profile according to:

$$N(x) = \frac{Q}{\sqrt{\pi Dt}} e^{-x^2/4Dt} \quad [1]$$

where D and t are the diffusion coefficient and diffusion time, respectively.

Ion implanted impurity atoms are in fact deposited in a shallow subsurface layer. Also, during diffusion the implanted atoms are free to diffuse out of the surface. Therefore, the resultant concentration profile cannot be expected to be truly gaussian. In this work, however, as shallow as possible implantation profiles were attempted. The implantation took place at low energies (~ 45 KeV) and the sample was orientated in such a way that the (111) direction made an angle of 8° to the incident beam to prevent channeling. In addition, the effects due to out-diffusion were assumed to be confined mainly in a region less than 0.1 microns from the surface. The deeper part of the concentration profile would still be a good approximation to the gaussian profile.

Determination of the Impurity Concentration Profile:

Both the sheet resistivity and concentration profiles of a diffused layer are essential in the determination of its characteristics. Of these

two, sheet resistivity can be measured directly, while the concentration of the impurity atoms must be calculated from the observed sheet resistivity values.

The sheet resistivity, ρ_S , is obtained using the four-point probe method (Valdes 1954; Uhlir 1955). The expression for ρ_S is given by:

$$\rho_S = \frac{V}{I} (\text{C.F.}) \quad [2]$$

where V is the measured voltage between the two inner probes and I is the known current between the two outer probes. The correction factor (C.F.) takes into account the finite dimensions of the sample (Smits 1958).

The sheet conductivity, $\sigma_S(x)$, of a subsurface layer of thickness $|x-x_j|$ and bulk conductivity, σ , is given by:

$$\sigma_S(x) = \int_x^{x_j} \sigma(x) dx .$$

Differentiating this expression,

$$\frac{d\sigma_S}{dx} = \sigma .$$

Since the sheet conductivity $\sigma_S \equiv 1/\rho_S$, the bulk resistivity is given by:

$$\rho = \left[\frac{d}{dx} \left(\frac{1}{\rho_S} \right) \right]^{-1}$$

where $\rho \equiv 1/\sigma$.

A typical plot of ρ_S versus x is shown in Fig. 3. In this sample 8.5×10^{14} B ions/cm² were implanted at about 40 KeV and diffused

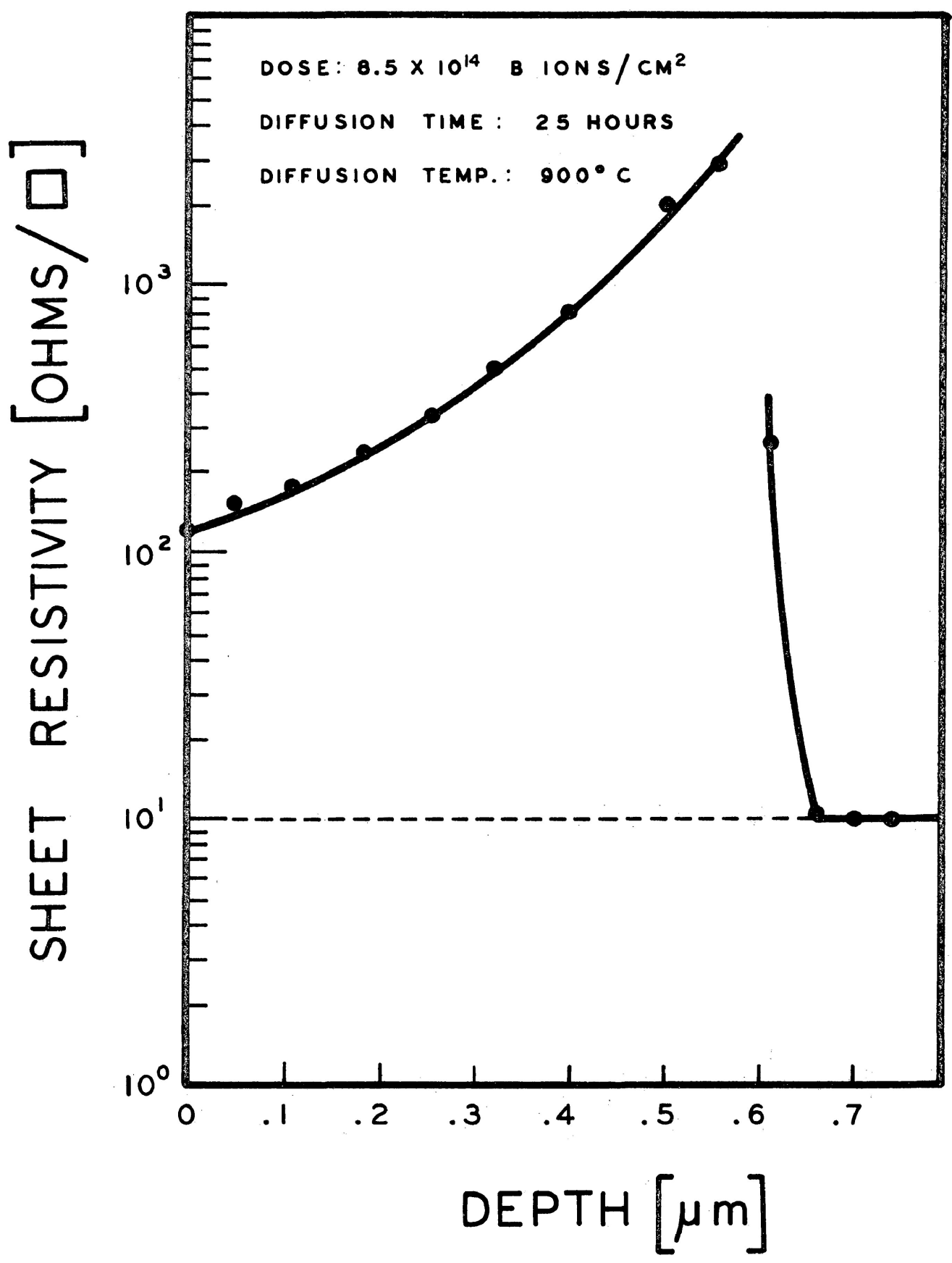


Figure 3. Sheet resistivity *versus* depth profile using a four point probe in conjunction with anodic oxidation profiling.

in a vacuum for 25 hours at 900° C. The horizontal broken line is the constant bulk resistivity. The inverse of the slope, $d/dx \left[1/\rho_S \right]$, at any point gives the value of the resistivity at that point. Using Irvin's data (Irvin 1962) of resistivity *versus* concentration, the value of the concentration was obtained for any point in the diffused profile. There is, however, some uncertainty in using Irvin's data in the damaged surface layer, since even after annealing the mobility may not be restored to the bulk value. In the diffused region the mobility of the sample is not affected by the implantation damage and Irvin's data is valid. The concentration profile corresponding to the resistivity *versus* depth graph (Fig. 3) is shown in Fig. 4. The constant background concentration in this sample was 1.2×10^{16} ions/cm³.

The described method of obtaining the concentration profile of a diffused layer was due to Tannenbaum (1961). Another more accurate method was put forward by Evans and Donovan (1967). This method improves the accuracy of the calculated concentration profile, especially in the region near the surface, where it is very difficult to determine the slope with any degree of accuracy.

Evans and Donovan began with the identity:

$$\frac{d\rho_S}{dx} = - \frac{1}{\rho_S} \frac{d \ln \rho_S}{dx}$$

and obtained:

$$\rho = \frac{0.4343 (\rho_S)}{\frac{d}{dx} (\log \rho_S)} .$$

This method still requires the slope, $d/dx (\log \rho_S)$, but here $\log \rho_S$ is easier to obtain than ρ_S where the slope was very small.

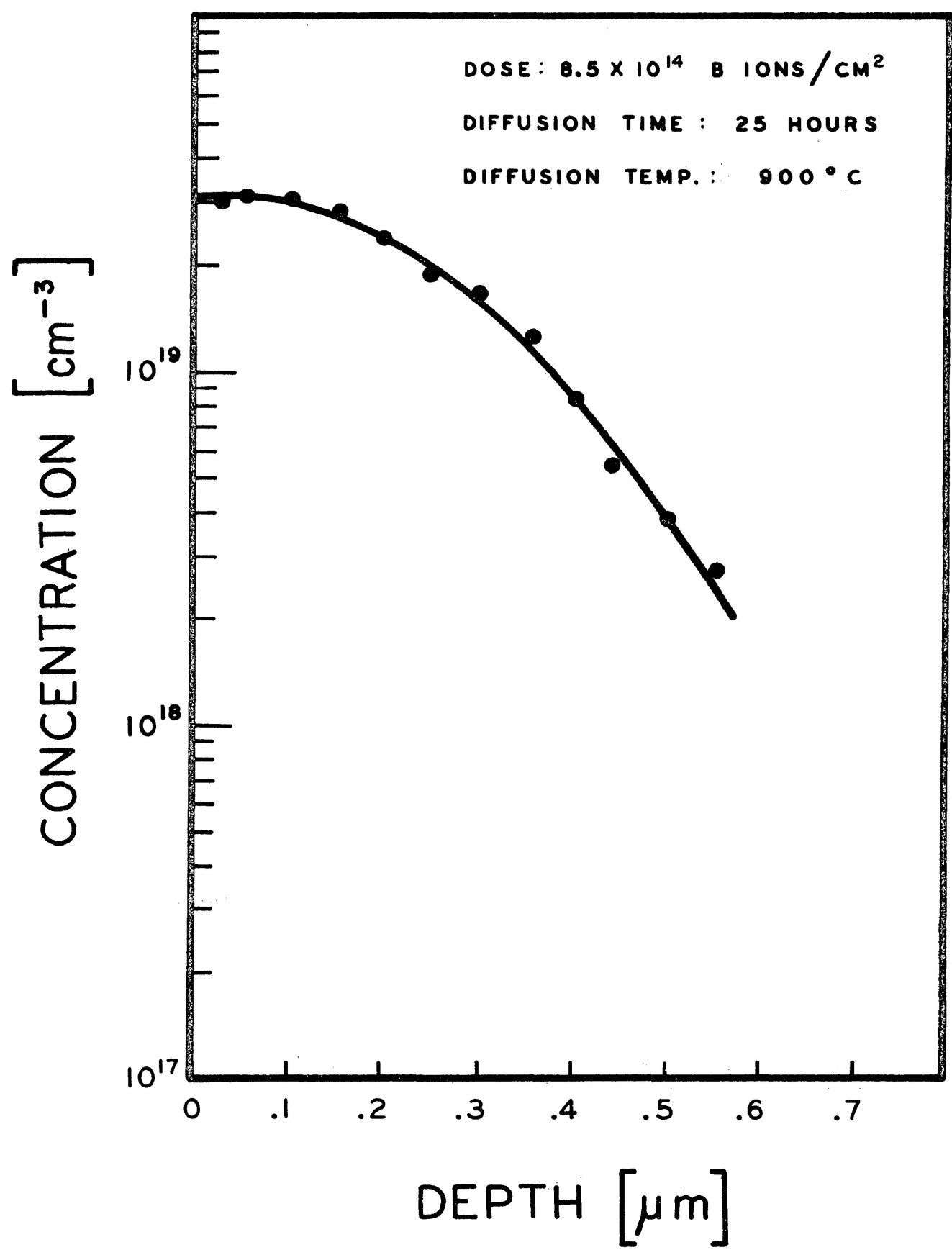


Figure 4. The concentration *versus* depth profile derived from the sheet resistivity profile in Fig. 3.

EXPERIMENTAL PROCEDURE

Sample Preparation:

Polished silicon slices of (111) orientation were obtained from Semi-Elements, Inc. The slices were of dimensions $10 \times 10 \times .5$ mm. The n-type silicon wafers were previously doped with 1.2×10^{16} phosphorus ions per cm^3 and had a resistivity of $0.5 \Omega\text{-cm}$. The p-type silicon wafers were doped with 1.9×10^{15} boron ions per cm^3 and had a resistivity of $7 \Omega\text{-cm}$. Before implantation the silicon wafers were cleaned in the following manner. After a short etch in HF and a methanol rinse, the samples were dipped in chloroform or in boiling methanol. This treatment appeared to leave a residue free surface, which was important, as the presence of a thin surface layer would affect the implantation process.

Implantation:

The silicon samples were then implanted at room temperature with the desired type of impurity. Fig. 5 is a schematic diagram of the system used for the implantation.

The ions were produced in a hot cathode discharge source and were accelerated by the electrodes 1 to 4 using a Universal Voltronics Model BAL-130-1.5 LU power supply, HV and a suitable divider chain. The beam then entered the magnetic field B for separation into its various mass components. After being bent through an angle of 30° along a path one meter in radius, the desired ion beam was collimated

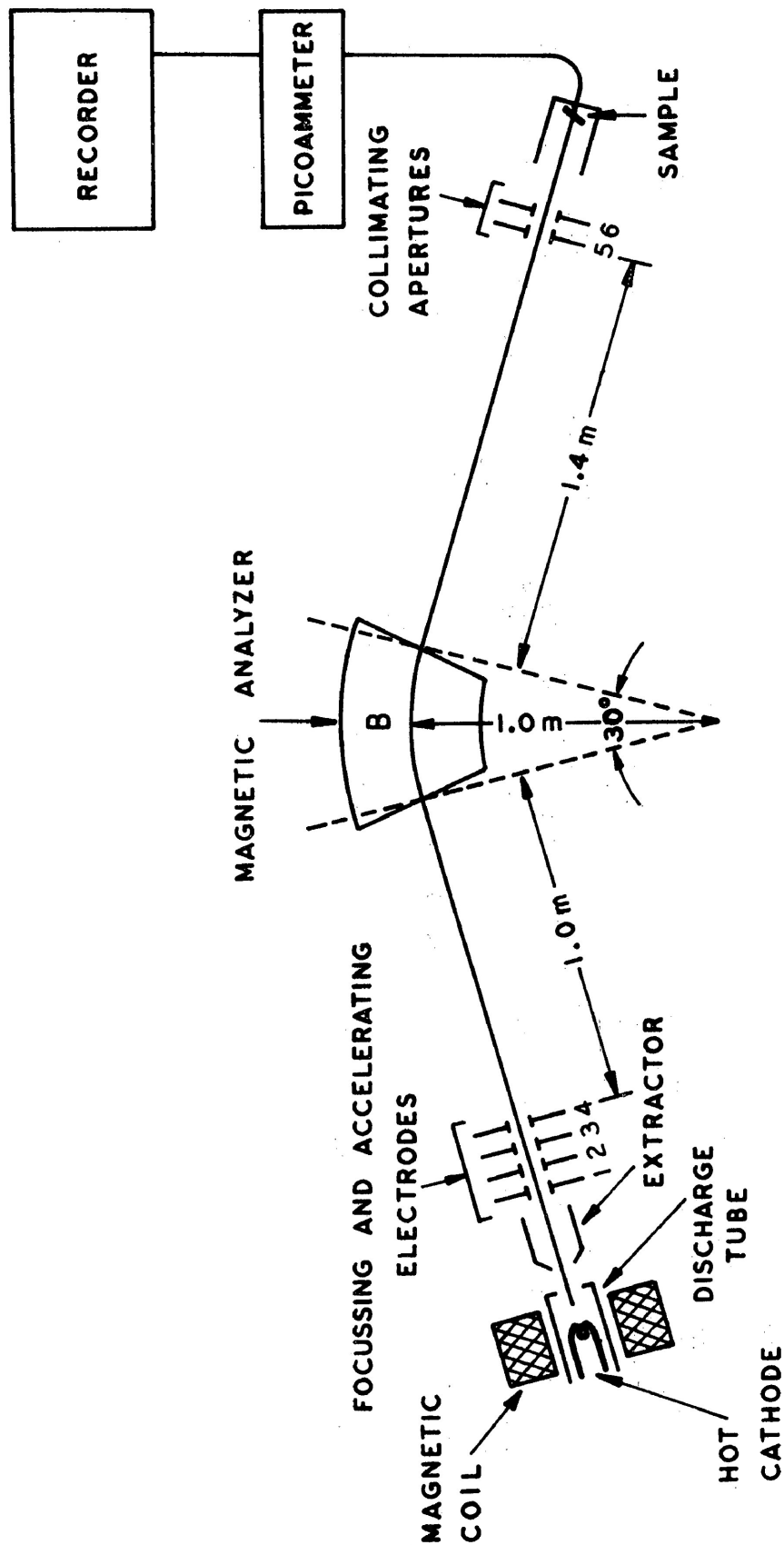


Figure 5. Schematic diagram of ion accelerator.

by apertures 4 and 5, then allowed to fall upon a silicon sample, s. The sample was held in a holder (see Fig. 6) at an angle of about 8° to prevent channeling. A long stainless steel tube was electrically connected to the sample holder to act as a Faraday cup to prevent any secondary emission from influencing the measured current. The ion current was measured with a Keithley Model 416 High Speed Picoammeter and recorded on a strip chart recorder.

Although the ion beam remained stationary relative to the sample during implantation, the implanted region was homogeneous. This was determined by making successive resistivity measurements across the face of the sample. However, in order to maintain consistency, the measurements were made in the same relative position on all samples.

The boron, phosphorus and arsenic ions were obtained by ionizing BCl_3 , PH_3 and AsH_3 , respectively. Current densities at the sample were of the order 10^{-7} to 10^{-9} amperes per square centimeter. The dose was determined by integrating the recorder tracing of the picoammeter output. The vacuum at the target end was maintained at approximately 1×10^{-6} torr during implantation and 1×10^{-7} torr with the source off.

Diffusion:

The silicon wafers were diffused in a Lindberg high temperature electric furnace in which was placed a 2" diameter quartz tube to protect the elements as well as to smooth out the temperature profile of the furnace. The temperature of diffusion was $900^\circ\text{C} - 1100^\circ\text{C} \pm 2^\circ\text{C}$ as measured by a platinum/platinum 13% rhodium thermocouple. The part of

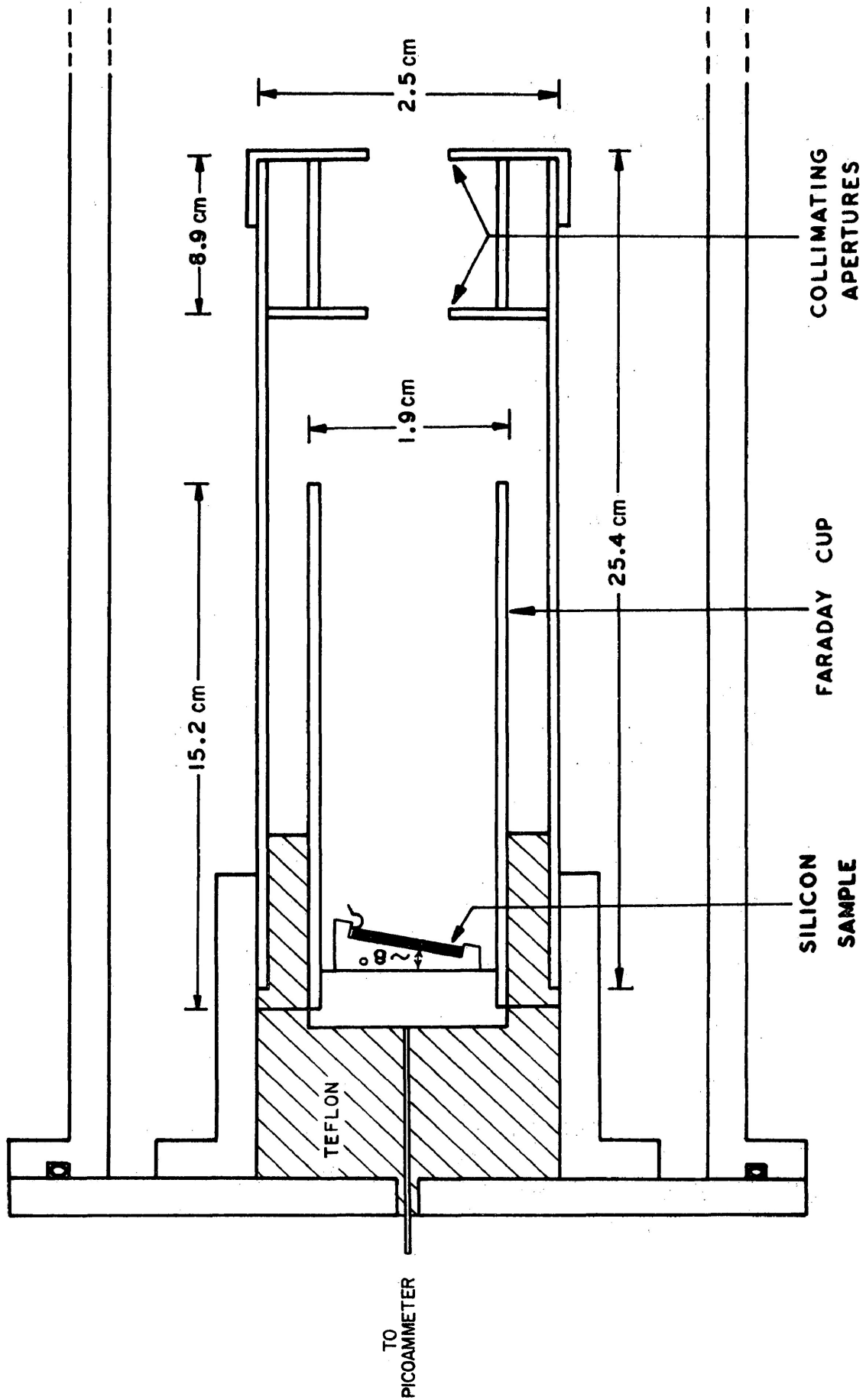


Figure 6. Diagram of target chamber and sample holder.

the furnace in which the slice was inserted had approximately 3 inches of constant temperature zone ($\pm 1^\circ\text{C}$). The silicon wafers were placed horizontally in a small quartz tube which was sealed off at about 10^{-7} torr.

Formation of the Mesa Structure:

Before sheet resistivity measurements were made on the diffused sample, it was desirable to isolate a region of definite dimensions on the surface. This was done in order to have an inversion layer of definite dimensions which was electrically isolated from the bulk material. The mesa was formed by first placing a piece of apiezon vacuum wax approximately $1 \times 4 \times .25$ mm on the silicon sample in the desired location. The sample was then heated on a hot plate until the apiezon just began to soften and then was removed to cool. The sample was then etched with a planar etch for about 15 seconds. This etch consisted of 15 parts HNO_3 , 5 parts CH_3COOH and 2 parts HF. As the planar etch had an etch rate of about 8 microns per minute, the etch time was controlled to ensure that all of the diffused region surrounding the mesa was removed. The region under the mesa was protected by the apiezon from attack by the etch. After etching, the masking material was removed by dissolving in trichloroethylene.

Sheet Resistivity Measurements:

The sheet resistivity was measured using a Signatone Model S-300 four point probe. Essentially, this consisted of four spring loaded

steel point contacts mounted in a line with a spacing of 0.025" between the contacts. A current (I) of about 50 microamperes, obtained from a dry cell battery, was passed through the outer two probes. The potential difference (V) across the inner probes was measured using a Hewlett-Packard Model 419A DC Null Voltmeter. The sheet resistivity, ρ_S , was then obtained using Eqn. [2].

Anodic Oxidation:

In order to measure the sheet resistivity throughout the entire diffused region, it was necessary to remove thin layers parallel to the junction one at a time. After each removal, the sheet resistivity of the remaining diffused region was measured with the four point probe. Removal was accomplished by an anodization process originally developed by Tannenbaum (1961). The experimental arrangement is shown in Fig. 7. In this process, the silicon sample acted as the anode in an electrolyte consisting of a 0.04 M solution of potassium nitrate in ethylene glycol (Przyborski, Roed, Libbert, Sarholt-Kristensen 1969). A platinum electrode was used as the cathode. The rate of formation of the oxide was about $4 \text{ \AA}/\text{volt}$ with the upper limit being about 500 V. Depending on the amount of material to be removed per single anodization, a constant voltage of 50 - 250 V was applied between the electrodes, resulting in oxide layers of 200 to 1000 \AA thick. The silicon dioxide layer was completely formed when the current through the system had decreased to essentially zero, because of the insulating properties of SiO_2 . The silicon sample was withdrawn from the electrolyte and the uniform colour of the oxide (which indicated a uniform thickness of oxide) was compared with

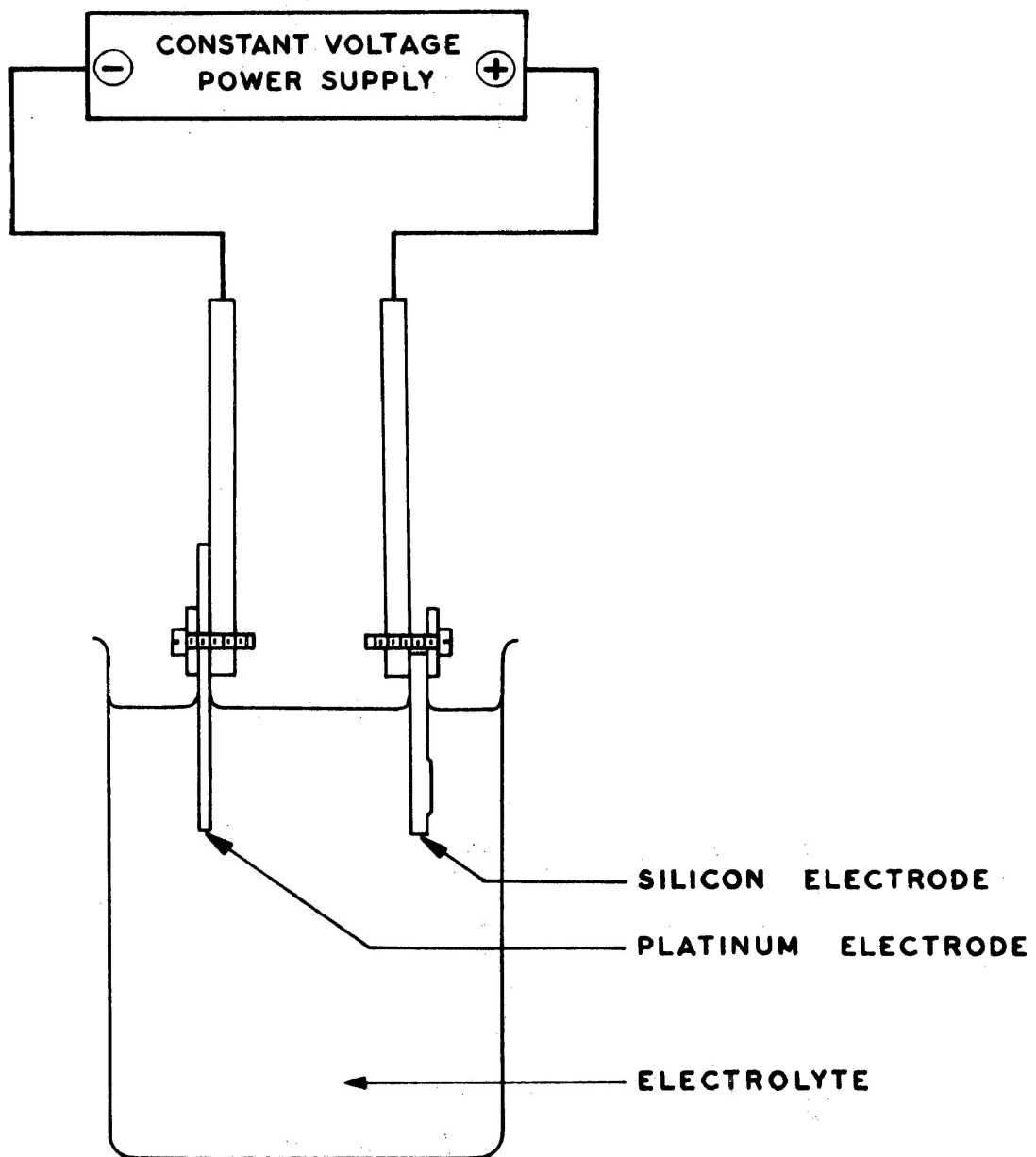


Figure 7. Diagram of anodic oxidation arrangement.

colour charts (Pliskin and Conrad 1964) to determine the thickness of the oxide layer obtained. The relative amount of silicon in the oxide layer was calculated and measured to be about 0.34. The measurement of the amount of silicon in the oxide layer was easily obtained. An interferometer was used to measure the thickness of the oxide layer formed. After the oxide was dissolved, the layer of silicon removed, as a result of the oxidation, was measured.

As the sensitivity of the colour change with the thickness varies over the spectrum, the most sensitive range was chosen, and, for the most part, the silicon was removed in increments of about 400 Å. The grown oxide layer was dissolved by dipping the silicon sample into HF. Concentrated HF readily dissolves SiO_2 but does not appreciably affect the silicon. The samples were rinsed in hot deionized water prior to the measurement of the sheet resistivity. This procedure was repeated until the entire diffused layer was removed.

Visual Measurement of Junction Depth:

In order to verify the value of the junction depth obtained by the anodic oxidation procedure, a separate piece of the sample silicon sample was polished at a shallow angle. The sample was mounted to an angled post with apiezon and supported vertically in a holder (see Fig. 8). The sample was lapped with 0.25 micron diamond paste, under a glass microscope slide. The procedure, which could be observed under a microscope, was continued until enough surface was lapped to expose the diffused layer on the angle. The sample was then removed from the post and a drop of staining solution consisting of 1 part HF, 3 parts HNO_3 and 20 parts

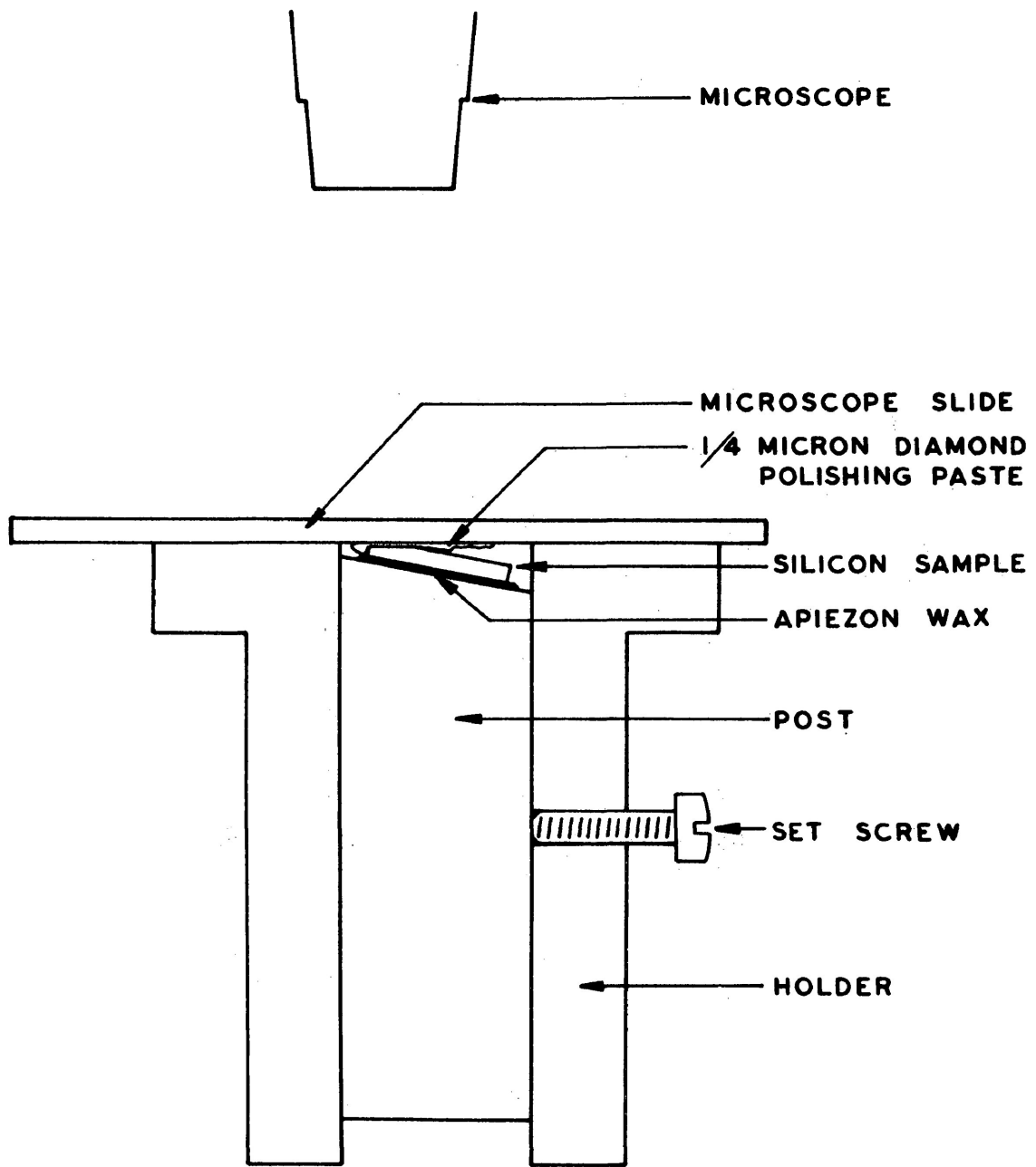


Figure 8. Diagram of angle polishing arrangement.

CH_3COOH was applied to the lapped surface, while viewing under a microscope. After a few seconds, when the p region turned dark compared to the n region, the sample was flooded with distilled water to terminate the process. A photograph was then taken in order to measure the diffused junction depths.

RESULTS AND DISCUSSION

The main purpose of the work was to determine the possibility of diffusing two different species of impurities at the same time. Before that was attempted, single diffusions were studied to determine their diffusion characteristics and to develop the experimental technique.

Impurities which were implanted into silicon acted as diffusion sources. The implanted layers were kept as shallow as possible so that the diffused concentration profile could be approximated by a gaussian distribution profile. With an implantation energy of 45 KeV boron ions were deposited to a depth of about 0.05 to 0.15 microns (Matthews 1971), while arsenic was deposited at an even shallower depth.

The diffusion of phosphorus and arsenic (n-type inducing impurity) and boron (p-type inducing impurity) were carried out in p- and n-type silicon, respectively. n-p and p-n junctions were obtained. Later arsenic and boron were implanted and diffused simultaneously in n-type silicon. The diffusion took place in a vacuum of 10^{-7} torr and no effort was made to prevent out-diffusion.

During diffusion only part of the implanted atoms became electrically active. Fig. 9 compares the per cent of the implanted dose that became electrically active for the elements boron, phosphorus and arsenic. The implanted dose was determined by integrating the implantation current *versus* time plots made during implantation and the number of electrically active ions present after diffusion was determined by integrating the obtained concentration *versus* depth curves. It can be

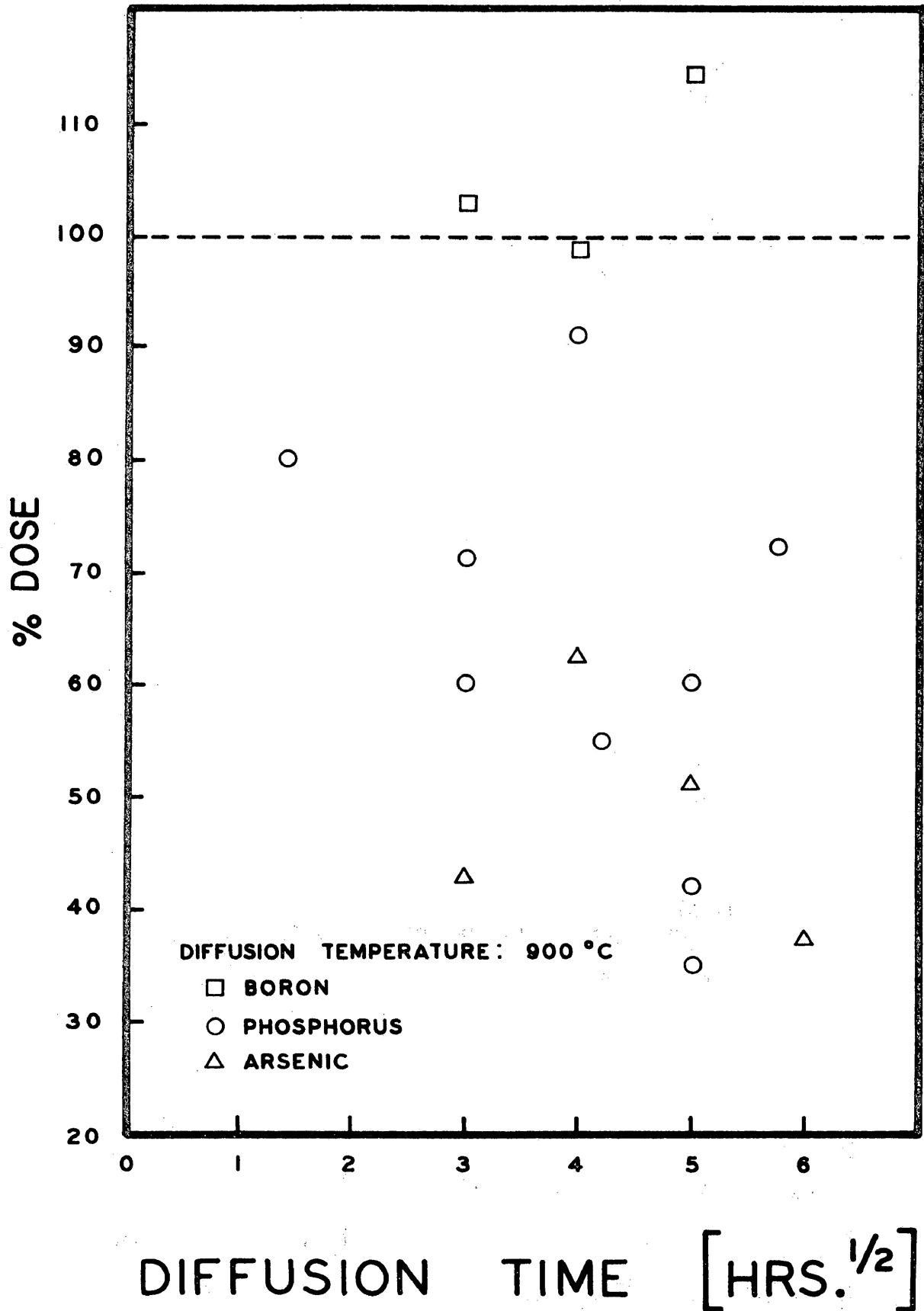


Figure 9. Per cent of implanted dose that became electrically active after a diffusion of 900°C for various diffusion times.

seen from Fig. 9 that on the average boron became completely active, while phosphorus and arsenic each became about 60% and 50% electrically active. An undetermined part of the implanted dose was probably lost through the surface because of out-diffusion. The considerable amount of scatter in the points was probably due to the fact that the samples were implanted with various doses and there may be some undetermined concentration dependent effects present.

After diffusion part of the sample was used for sheet resistivity measurements, while the other was angle lapped and stained to reveal the p- and n-type layers. Fig. 10a shows a p-type silicon sample which was implanted with 1.2×10^{15} phosphorus ions per square centimeter at 45 Kev, diffused, angle lapped at 1.4° and stained. The p-type substrate turned dark, while the n-type phosphorus layer remained unaffected. In this sample, the junction depth is 1.5 microns. A doubly implanted sample which was diffused for 4 hours at 1025°C , angle lapped at 1.4° and stained is shown in Fig. 10b. The first layer of arsenic had diffused to a depth of 0.4 micron, while the p-type boron, which had stained dark, had diffused to a depth of 1.0 micron. In all cases, the junction boundaries were parallel to the surface except near the implanted edges where there was rounding. These photographs were made with an optical microscope using vertical illumination.

Electrical measurements were made on another piece of the same sample in order to verify the results obtained from the angle lapping and staining technique. Fig. 3 shows a typical sheet resistivity *versus* depth profile of a diffused sample. In this figure, the logarithm of sheet resistivity in ohms per square was graphed as a

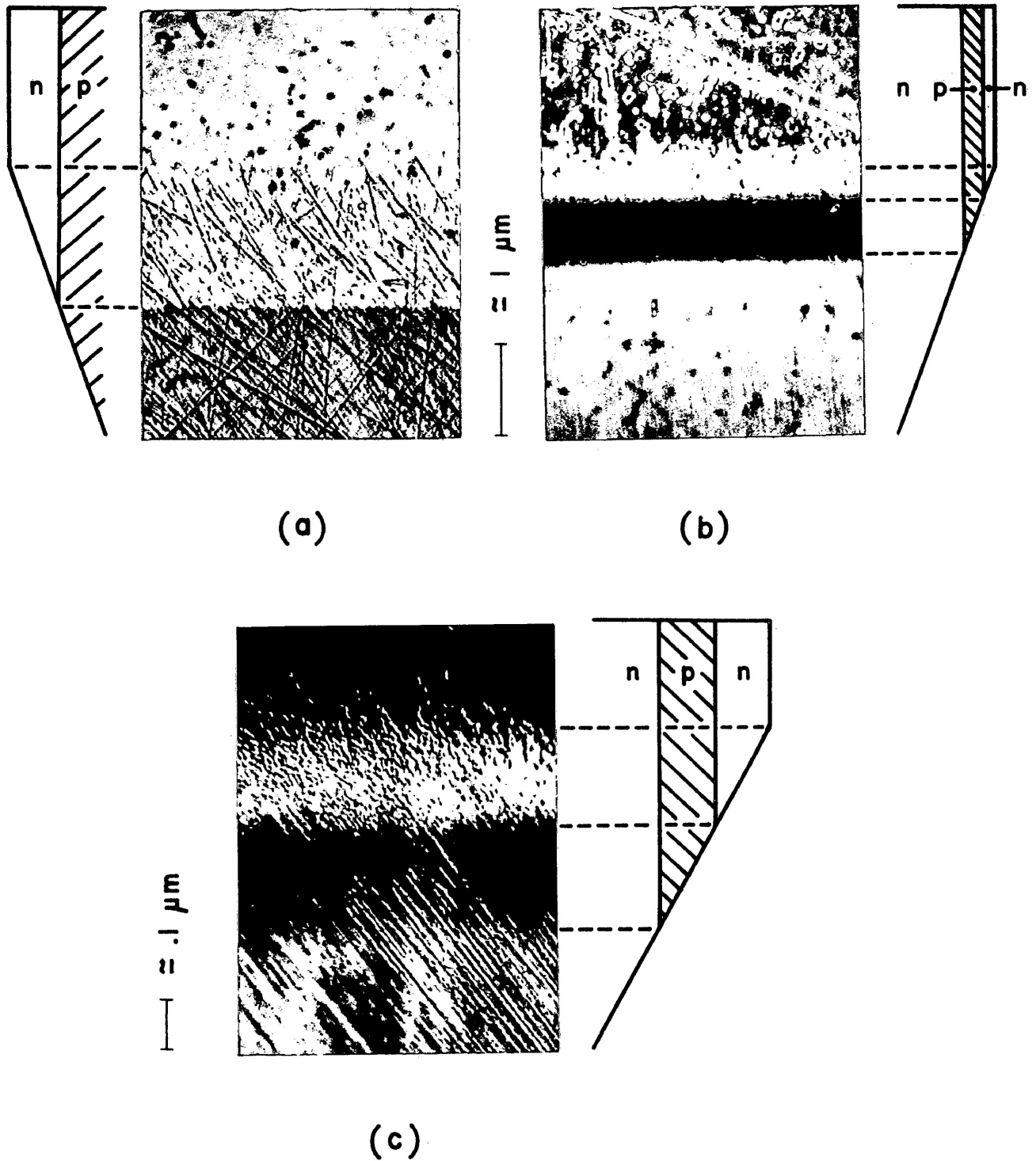


Figure 10. Angle-lapped and stained samples showing the carrier type distribution. The dark regions are p-type silicon.

function of the distance from the initial surface in microns. This sample was implanted with 8.5×10^{14} boron ions per square centimeter at room temperature and diffused for 4 hours at a temperature of 900° C. The four point probe sheet resistivity measurements were made in conjunction with the anodic oxidation profiling technique. The sheet resistivity values were calculated using Eqn. [2]. The corresponding concentration *versus* depth profile is shown in Fig. 4. This is a semi-logarithmic graph of the number of boron ions per cubic centimeter *versus* the depth in microns. The concentration profile was obtained from the sheet resistivity curve using the method of Evans and Donovan (1967).

The B and As diffused junction depths behave linearly as expected from Eqn. [1]. The extrapolated junction depths for zero diffusion time all agree well with the LSS theory (Lindhard, Scharff and Schiøtt 1963), except P. No explanation is given for the anomalous behaviour of the P implants.

As arsenic and boron had an appreciable difference in diffusion rate, they were selected for double diffusion. Both doping impurities were then studied in order to obtain plots of junction depth *versus* diffusion temperature for various implanted doses (see Figs. 12 and 13). In both graphs, the junction depths obtained by anodic oxidation profiling and

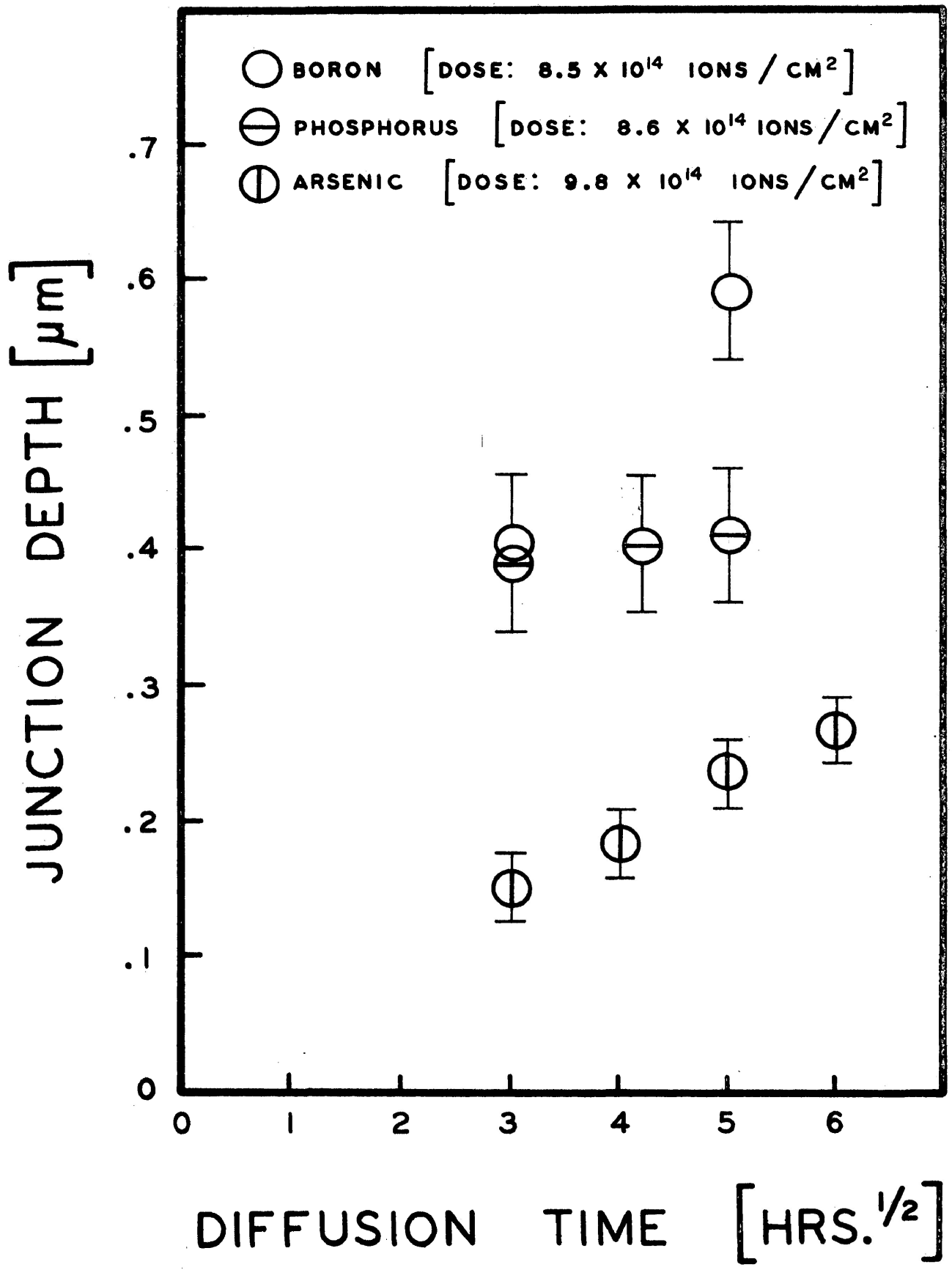


Figure 11. The junction depths obtained by the anodic oxidation - sheet resistivity method, after a diffusion at 900°C for various diffusion times.

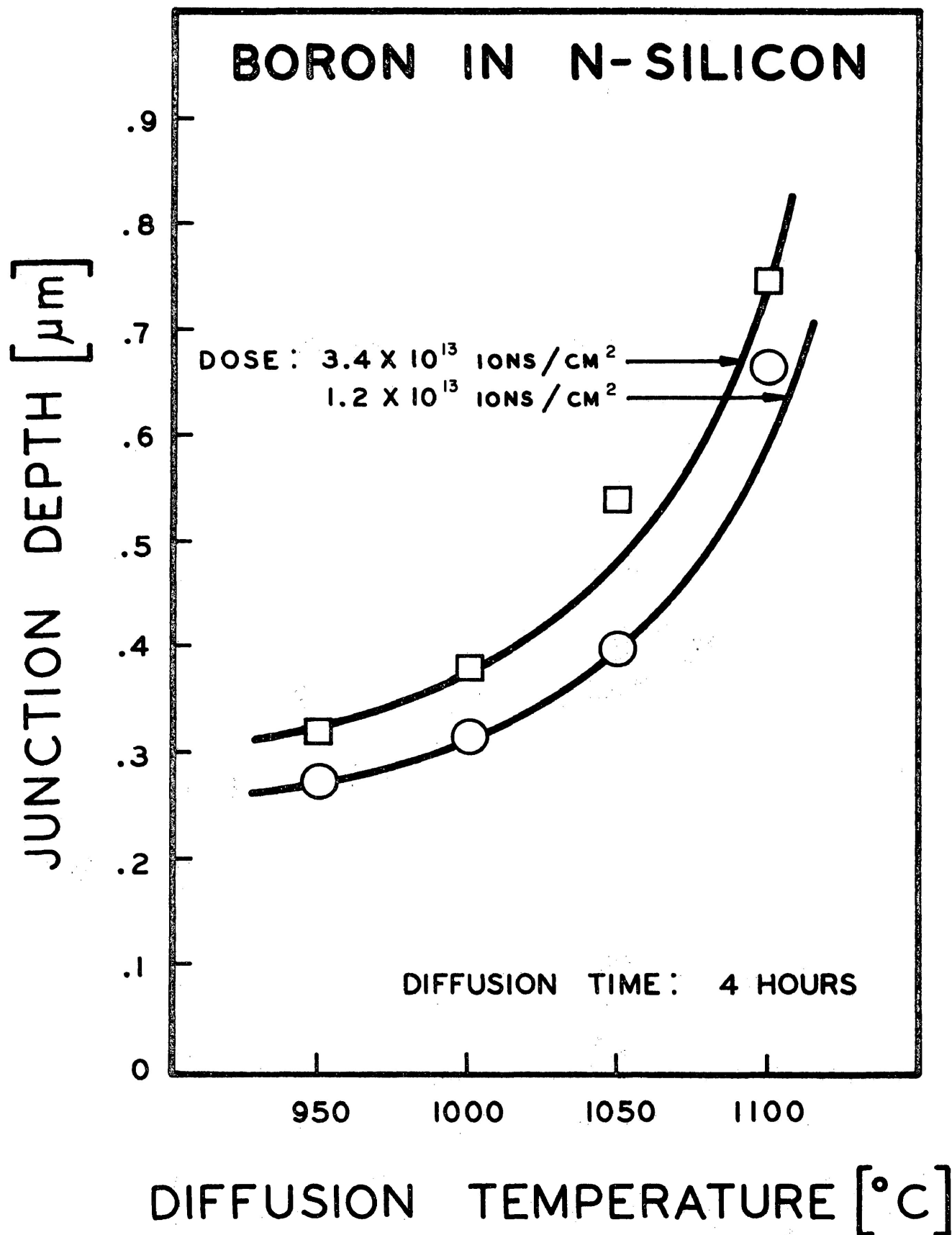


Figure 12. Junctions depths for boron diffusions in n-type silicon obtained by anodic oxidation profiling after a diffusion time of 4 hours at various diffusion temperatures.

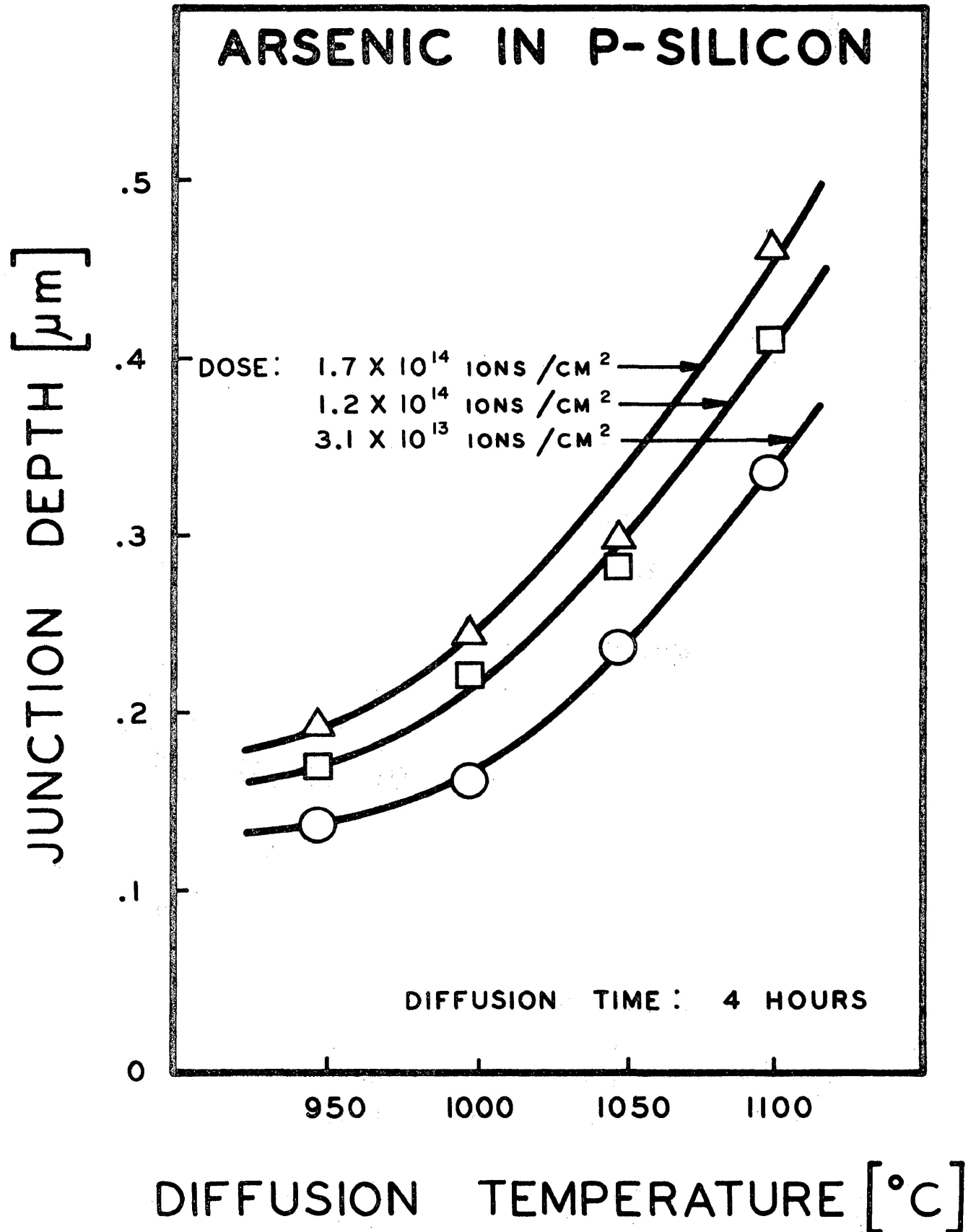


Figure 13. Junction depths for arsenic diffusions in p-type silicon obtained by anodic oxidation profiling after a diffusion time of 4 hours at various diffusion temperatures.

sheet resistivity measurements were plotted *versus* the diffusion temperature in degrees centigrade. Twenty samples were used in the study. Each of the two boron and three arsenic implanted wagers was cut into four pieces and each diffused at 950, 1000, 1050 and 1100°C.

Using the curves in Figs. 12 and 13, it was possible to gain a good idea of the implanted doses and diffusion temperatures required to produce a pronounced double junction.

A typical sheet resistivity *versus* depth plot of a doubly implanted and diffused sample is shown in Fig. 14. This particular n-type silicon sample was implanted with 1.0×10^{14} arsenic ions per square centimeter and 1.5×10^{13} boron ions per square centimeter. The silicon wafer was diffused at 1025°C for 4 hours. The sheet resistivity values were obtained using the four point probe in conjunction with anodic oxidation profiling. The dotted lines in the resistivity profile indicate extrapolations based on the obtained measurements. The horizontal broken line is the sheet resistivity of the constant background concentration. Data points below the background resistivity are attributed to some unknown effect. The corresponding concentration profile is shown as the solid line in Fig. 15. Dotted lines indicate the extrapolated curve. It was not possible to obtain reasonable concentration profiles in the vicinity of the junctions, as sheet resistivity measurements here are difficult to interpret. For example, near the second junction the inversion layer of sheet resistivity of about $10^4 \Omega$ is over a comparatively conducting bulk material of sheet resistivity of $10^1 \Omega$. In this situation the correction factor in Eqn. [2] becomes very critical if the thickness of the layer is small compared with the probe spacing (Hunter 1970).

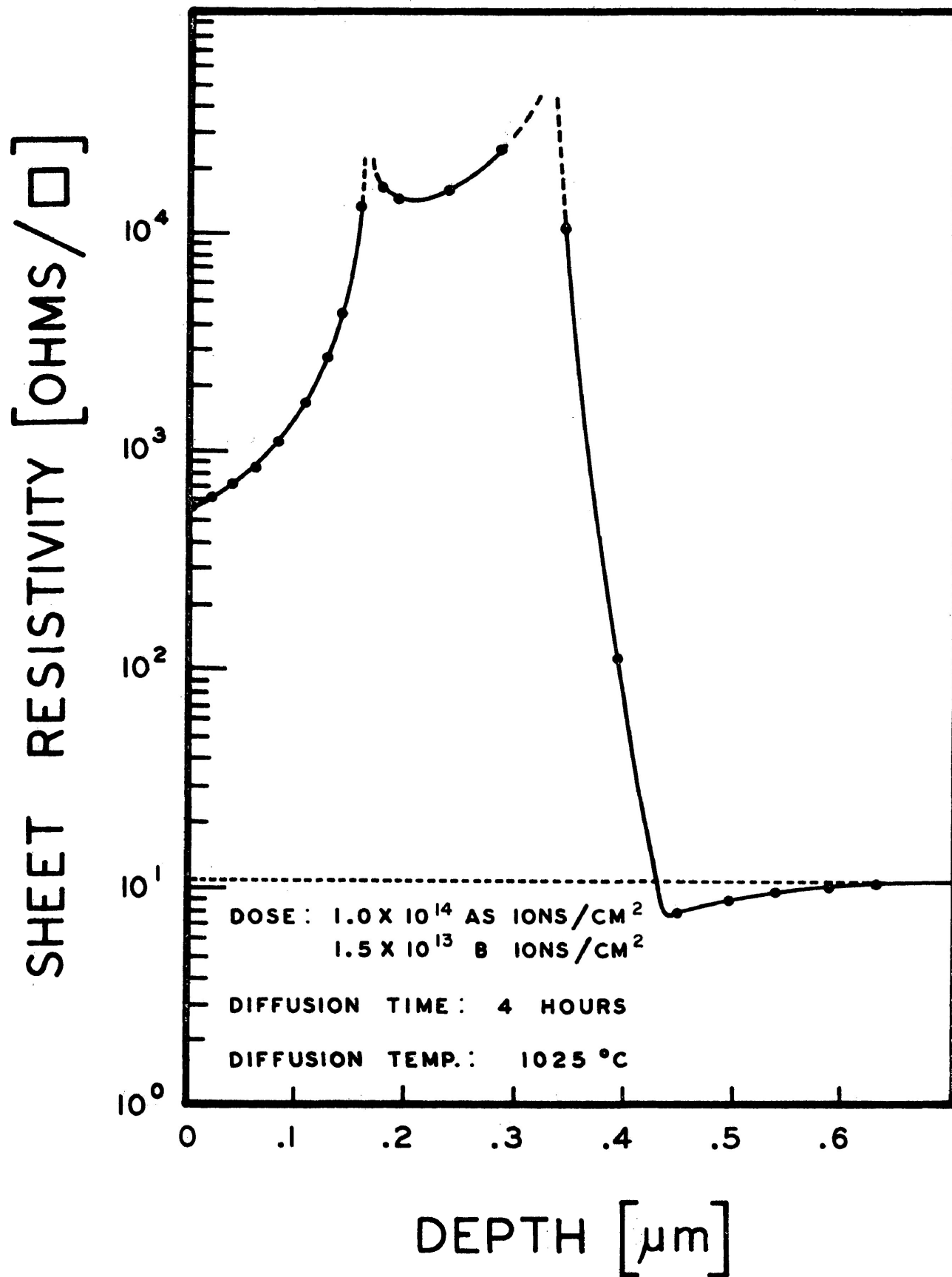


Figure 14. Typical sheet resistivity *versus* depth profile of a double diffusion of arsenic and boron in n-type silicon. The measurements were obtained using the four point probe and anodic oxidation arrangement.

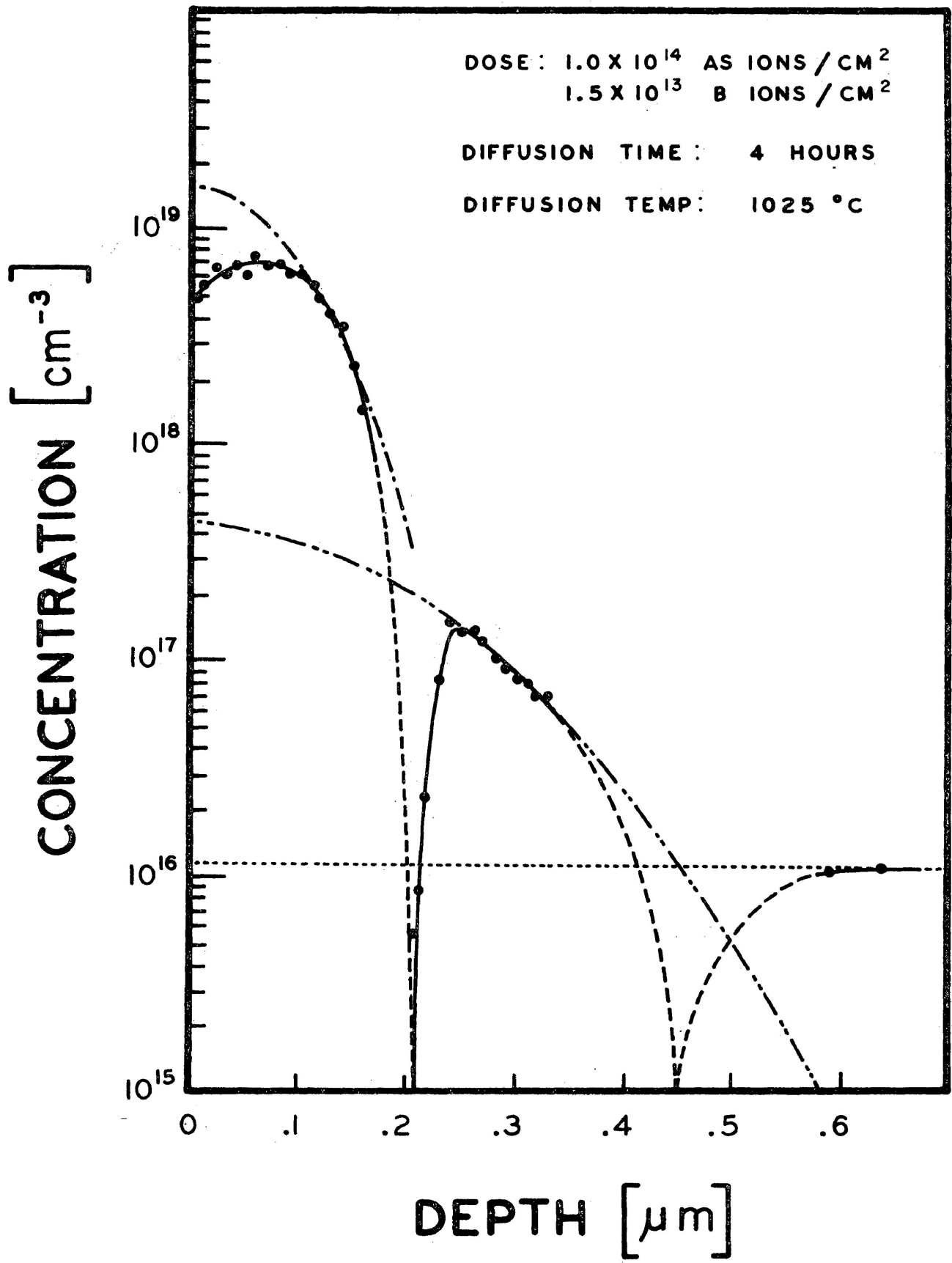


Figure 15. The concentration profile derived from the resistivity profile in Fig. 14. The best fitting gaussian curves are represented by dot and dash curves.

In Fig. 15 the dash-dot curve is the best fit of a gaussian distribution (Eqn. [1]) to the observed arsenic profile in the range 0 to 1.7 microns. The dash-double dot curve is the best fit for the observed boron profile in the range 0.24 to 0.34 micron. The gaussian curve given by Eqn. [1] was fitted to the observed concentration curves by a trial and error method using an APL computer terminal. First, however, the approximate values of the diffusion coefficient (D) and implanted dose (Q) for each curve were obtained using a linear regression program. As the decrease in concentration near the surface in some of the concentration profiles was rather pronounced, the fitted profile was influenced to a certain degree by these points, and as a result the fitted curve was lower than desired. Using the values of D and Q obtained from the linear regression analysis, they were adjusted by trial and error at an APL terminal until the fitted curve most closely approximated the obtained concentration curve in the region away from the surface.

For arsenic, near the surface, the fitted curve differs appreciably from the observed curve. This can be explained partly by the fact that there is a maximum in the concentration profile at some depth below the surface for ion implanted and annealed samples (Matthews 1971). As arsenic diffuses slowly, this shape of concentration profile could still exist after a limited diffusion. Also, the decrease of concentration near the surface could be due to some out-diffusion of arsenic into the vacuum during the diffusion process. For boron, although the possibility for comparison between the fitted and observed curve is limited, the corresponding calculated value of D from Fig. 15 agrees exactly with other boron samples and the uncertainty in determining the value of Q was no

more than $\pm 10\%$.

The obtained values of D and Q from Fig. 15 are listed in Table 1. Here it can be seen that the obtained values of Q agree with the implanted doses within a factor of about 0.6. For arsenic, the larger value of Q results from fitting a gaussian curve to the observed profile. The gaussian distribution, which has a maximum at the surface, was fitted so that it corresponded to the arsenic concentration curve in the region deeper than the concentration maximum. This results in some discrepancy between the theoretical and observed curves in the region close to the surface. The obtained diffusion coefficients of both diffusing impurities agree very well with the single implanted and diffused samples in Fig. 17.

The angle-lapped and stained photograph of the same sample which was electrically analyzed in Figs. 14 and 15 is shown in Fig. 10c. This photograph was taken with a scanning electron microscope at about 20° from the normal. It can be seen that the surface has stained dark, although the top layer being arsenic should not have stained at all. This effect was observed in various degrees in all double implanted and diffused samples, but the cause of this was not determined. In spite of this, the junction depths obtained from angle-lapping and staining compare very favourably with the electrical measurements. In Fig. 10c the diffused arsenic and boron depths are 0.20 micron and 0.41 micron, respectively, while from the concentration *versus* depth profile in Fig. 15 the junctions depths are 0.21 micron and ~ 0.45 micron.

These results also compare favourably with another sample treated under the same conditions. The junction depths here were 0.21 and ~ 0.48 micron for arsenic and boron, respectively.

TABLE 1

Comparison of the implanted dose and parameters of the best fitting gaussian profiles for the doubly implanted and simultaneously diffused sample in Fig. 15.

	Implanted Dose (Ions / cm ²)	Q (Ions / cm ²)	D (1025°C) (cm ² / sec)
As	1.0×10^{14}	1.6×10^{14}	2.0×10^{-15}
B	1.5×10^{13}	9.4×10^{12}	1.0×10^{-14}

By comparing the above results with the interpolated results of Figs. 12 and 13, it can be seen that the arsenic junction depth for single diffusion is the same as for double diffusion. For boron, the junction depth is about 20% deeper for double diffusion than for single diffusion. As the experimental error for this work was assumed to be 20%, no definite conclusions were made regarding the interaction of the diffusing impurities for the limited number of samples analyzed.

The diffusion coefficient for each single impurity diffusion was found by fitting a gaussian curve to the observed concentration profile. Fig. 16 shows an example of a series of concentration profiles of boron implanted silicon wafers. The implanted silicon wafer, with a dose of 3.4×10^{13} boron ions per square centimeter, was cut into 4 pieces and each was diffused at 950, 1000, 1050 and 1100°C for 4 hours. The concentration profiles from the corresponding measured sheet resistivity profiles were calculated. The values of D and Q were then obtained from the best fitting gaussian curve (Eqn. [1]) using APL.

The rather large amount of scatter in the points of Fig. 16, especially near the surface of the sample, was attributed to the difficulty in determining the incremental slopes of the corresponding sheet resistivity curves. If the horizontal increment on the sheet resistivity curve is large, then the slopes along the curve are more accurately determined and there is less scatter in the calculated points of the concentration profile (see Fig. 4). However, this also causes a corresponding decrease in the resolution of the curve.

The values of D and Q obtained from fitting gaussian curves to the concentration profiles in Fig. 16 are listed in Table 2. It can be seen

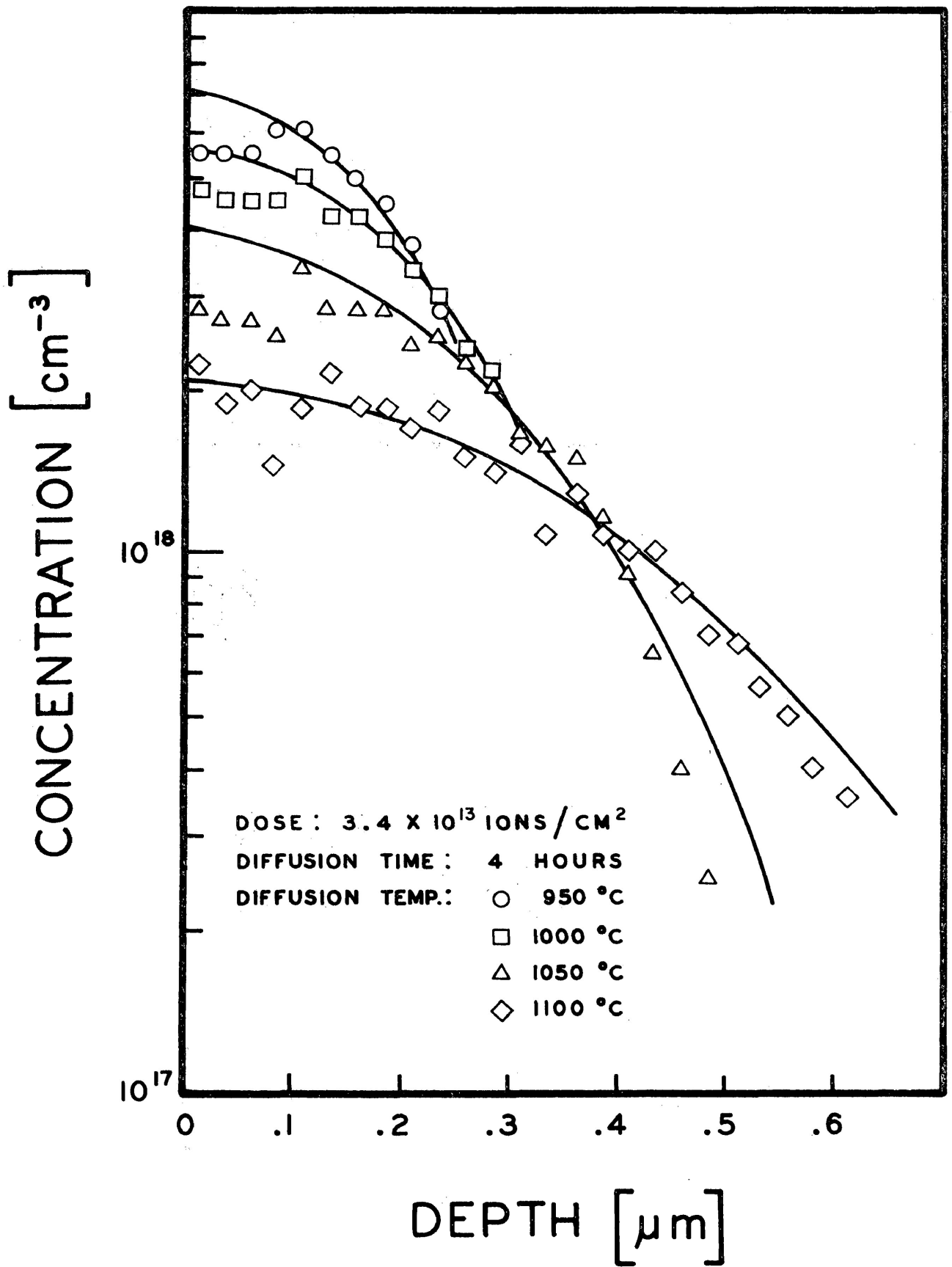


Figure 16. The experimental points and calculated profiles for boron after a diffusion of 4 hours.

TABLE 2

Comparison of the implanted dose and parameters of the best fitting gaussian profiles for the boron concentration profiles in Fig. 17.

Implanted Dose (Ions/cm ²)	Diffusion Time (°C)	Diffusion Temperature (Hours)	Q (Ions/cm ²)	D (cm ² /sec)
3.4×10^{13}	950	4	1.5×10^{14}	1.0×10^{-14}
3.4×10^{13}	1000	4	1.45×10^{14}	1.5×10^{-14}
3.4×10^{13}	1050	4	1.3×10^{14}	2.0×10^{-14}
3.4×10^{13}	1100	4	9.5×10^{13}	4.2×10^{-14}

that the obtained values of Q are larger than the implanted dose. This is due to the dissimilarity between the fitted gaussian and observed concentration profiles in the region less than about 0.1 micron from the surface. For larger diffusion times, the concentration maximum, which occurs just below the surface, decays and the profile more closely approximates the gaussian curve. At the same time Q approaches the implanted dose.

The values of D obtained by fitting gaussian curves to boron and arsenic samples are shown in Fig. 17. In this graph, the diffusion coefficients of B and As were graphed as a function of the inverse of temperature in degrees Kelvin times 10^3 , along the bottom of the graph, and diffusion in degrees centigrade along the top of the graph. All of the arsenic and boron samples which were implanted at various doses were diffused for 4 hours. The values of D obtained are in general agreement with the rather wide range of published values. The results of Fuller and Ditzenberger (1956) are included here for comparison. The solid lines represent their observed values of the diffused coefficients of boron and arsenic. The broken line is an extrapolation of the given arsenic diffusion coefficient curve.

Sources of Errors and Accuracy:

The resistivity measurements were made using a four point probe. These measurements were reproducible to within $\pm 5\%$. This holds until the anodization has proceeded to within about 1000 \AA of the junction. At this point, the sheet resistance is generally in the range of $10^3 \Omega/\text{square}$ and the measurements have a tendency to drift somewhat

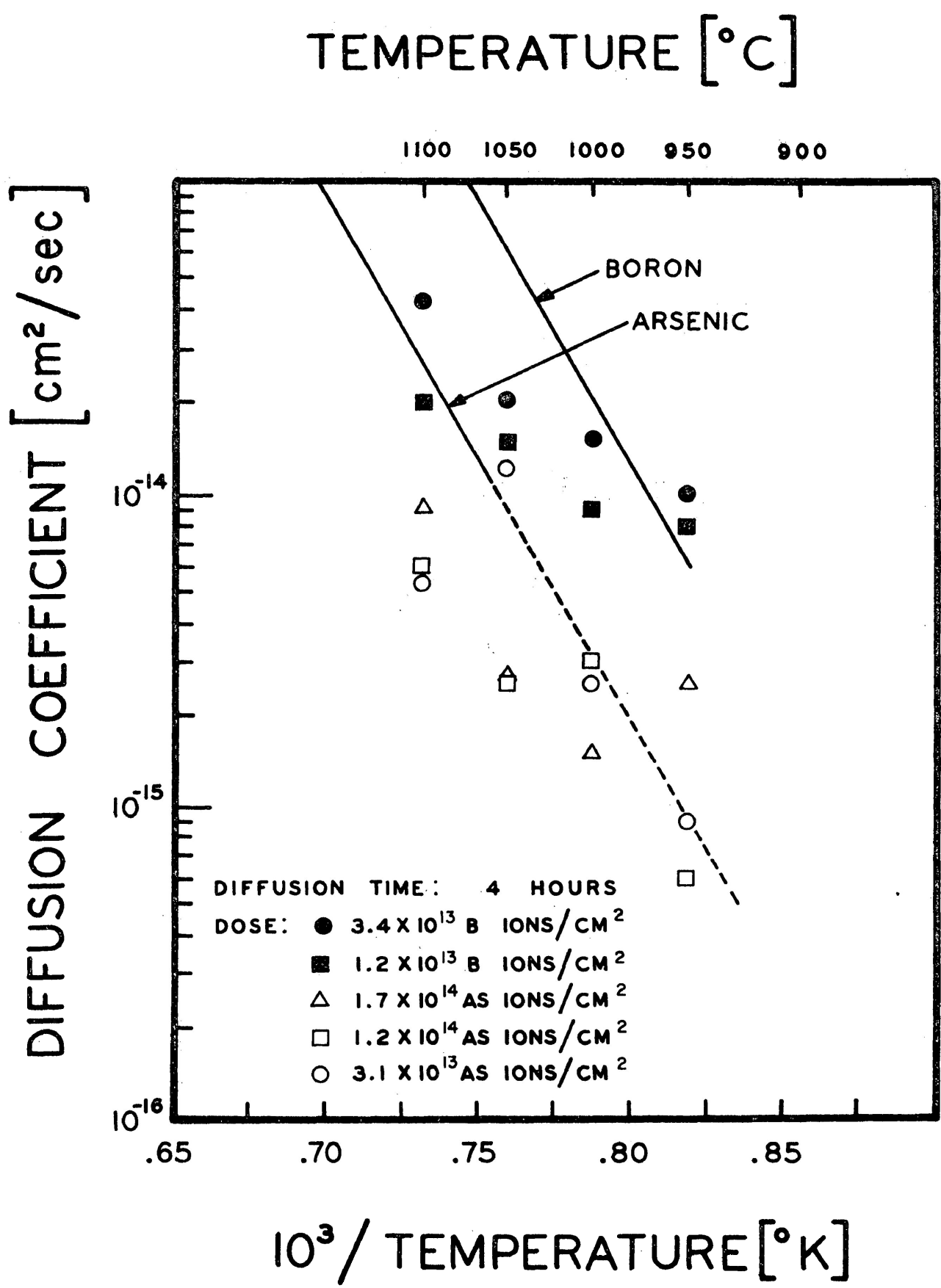


Figure 17. The diffusion coefficients for single impurity diffusions at various diffusion temperatures, obtained by fitting the gaussian distribution profile to the obtained results. The curves are due to Fuller and Ditzenger (1956).

with a reproducibility of approximately 10%. Since it is only the last two or three measurements on a given sample that are subject to drift, an accuracy of 5% in the resistivity measurements can be safely claimed.

Some of the causes of such a decrease in reproducibility of the sheet resistivity measurements near the junction are the shorting of the bulk material beyond the junction, the penetration of the four point probes beyond the surface, and the non-uniformity in the formation of the oxide layer during anodic oxidation.

The junction acts as an insulating barrier, separating the inversion layer from the bulk. This assumption is reasonable if the area of investigation is far from the junction. As the junction is approached the effect of the bulk material becomes felt. This effect may be described by a leakage current through the junction.

In placing the probes on the surface of the diffused sample, some load is applied to each of the four points of the probes. Although the yielding pressure of silicon is slightly higher than that of steel, the probe points probably penetrate the surface. Thus, the resistivity being measured is not that of the surface, but of a layer very near the surface.

The original surface and the junction plane may not be perfectly flat and also the method of material removal may not be uniform. Therefore, some regions may show the bulk material before other regions.

Errors are introduced in determining the thickness of the oxide layer removed. In the estimation of the colour of the oxide, an error of $\pm 5\%$ of the true oxide thickness was assumed.

Comparison of the junction depth measured by the angle polishing and staining technique and the anodic oxidation technique gave about 10% difference.

All the data form smooth curves within the given error limits. Considering the overall error, including uncertainties in calibration constants as well as uncertainties in the measurement of slopes, the experimental data are believed to be accurate to within 20%.

CONCLUSIONS

The implantation and diffusion of boron, phosphorus and arsenic in silicon has been carried out in order to obtain some knowledge of the diffusion phenomenon. The possibility of implanting and diffusing two impurities simultaneously has been demonstrated, and within experimental error there is no interaction evident between the two diffusing impurities.

The diffusion temperature of 900°C was high enough to anneal the damage caused by implantation and to electrically activate the implanted atoms (Baron, Shifrin, Marsh, Mayer 1969). By calculating the area under the concentration profile and comparing it with the implanted dose, it was determined that for single diffusions approximately 50% of the arsenic ions, 60% of the phosphorus ions and all of the boron ions became electrically active after diffusion. For an implantation energy of 45 KeV, the implanted ions formed a concentration maximum about 0.05 to 0.15 micron below the surface (Kleinfelder, Johnson, Gibbons 1968). After limited diffusion, a concentration maximum existed here and is thought to be due to the remnants of the implanted profile. Also an undetermined amount of the implanted impurity near the surface could have escaped into the vacuum during diffusion, helping to create this concentration maximum. The values of D obtained from the concentration curves were within the wide range of values quoted in the literature. The values of Q (implanted dose) that were obtained from fitting gaussian curves to the observed concentration profiles were consistently higher than those which were actually implanted. This arises from the

discrepancy between the observed concentration profile and the gaussian profile in the region less than 0.1 micron from the surface. The difference was most evident in arsenic diffused concentration profiles and least in boron profiles. It was concluded that the gaussian profile is not a good approximation to ion implanted and diffused concentration profiles near the surface.

The technique of double implantation and simultaneous diffusion, described in this work, has the potential of being of practical use in the fabrication of complex semiconductor structures requiring depths larger than those obtained by implantation alone.

REFERENCES

- Baron, R., Shifrin, G.A., Marsh, O.J. and Mayer, J.W., *Journal of Applied Physics* 40, 3702 (1969).
- Baron, R., Shifrin, G.A., Marsh, O.J. and Mayer, J.W., *Solid State Electronics* 13, 317 (1970).
- Carslaw, H.S. and Jaeger, J.C., *Conduction of Heat in Solids* (Oxford University Press: Fair Lawn, New Jersey, 1948).
- Crank, J., *The Mathematics of Diffusion* (Oxford University Press: Fair Lawn, New Jersey, 1956).
- Duffek, E.F., Benjamini, E.A. and Mylroie, C., *Electrochem. Tech.* 4, 75 (1965).
- Duncan, D.M. U.S. Patent No. 3, 664, 896 (1972).
- Evans, R.A. and Donovan, R.P., *Solid State Electronics* 10, 155 (1967).
- Fuller, C.S. and Ditzenberger, J.A., *Journal of Applied Physics* 27, 544 (1956).
- Hunter, L.P. (ed.), *Handbook of Semiconductor Electronics* (McGraw-Hill: New York, 1970).
- Irvin, J.C., *Bell Syst. Tech. J.* 41, 387 (1962).
- Kleinfelder, W.J., Johnson, W.S. and Gibbons, J.F., *Can. J. Phys.* 46, 597 (1968).
- Lindhard, J., Scharff, M. and Schiøtt, H.E., *Kgl. Danske Videnskab Selskab, Mat.-Fys. Medd.* 33, 14 (1963).
- Matthews, M.D., *Phys. Letters* 37A, 257 (1971).
- Ohl, R., *Bell Syst. Tech. J.* 31, 104 (1952).

- Pliskin, W.A. and Conrad, E.E., IBM J. Res. Dev. 8, 43 (1964).
- Przyborski, W., Roed, J., Lippert, J. and Sarholt-Kristensen, L., Rad. Effects 1, 33 (1969).
- Shewmon, P.G., *Diffusion in Solids* (McGraw-Hill: New York, 1963).
- Smits, F.M., Bell Syst. Tech. J. 37, 711 (1958).
- Tannenbaum, E., Solid State Electronics 2, 123 (1961).
- Uhlir, A., Jr., Bell Syst. Tech. J. 34, 105 (1955).
- Valdes, L.B., Proc. I.R.E. 42, 420 (1954).
- Wagner, S., J. Electrochem. Soc. 119, 1570 (1972).